International Journal of Engineering Research and Technology. ISSN 0974-3154 Volume 10, Number 1 (2017)

ZnO-based photoelectrodes for dye sensitized solar cellvia modified successive ionic layer adsorption and reaction route

M. A. Gaikwad[a,c], M. P. Suryawanshi[b], S.P. Desai[a], A. V. Moholkar[a*]

[a]*Thin Film Nano Materials Laboratory, Department of Physics, Shivaji University, Kolhapur 416-004, M. S., India.*

[b]*Optoelectronics Convergence Research Center, Department of Materials Science and Engineering, Chonnam National University, 300,Yongbong-Dong, Buk-Gu, Gwangju 500-757, South Korea.*

[c]*Department of Physics, D. Y. Patil College of Engineering & Technology, Kasaba Bawada, Kolhapur-416006, M. S.,India*

Abstract

The modified successive ionic layer adsorption and reaction (M-SILAR) method is employed to deposit zinc oxide (ZnO) thin films without prior seed layer treatment. The method has been modified in concerns with the anionic and the rinsing bath. The anionic bath of diluted H_2O_2 is kept at 353 K, whereas traditional rinsing bath has been replaced by the ultrasonic rinsing. The modifications have led to increase in the chemical stability of an anionic bath. The impact of M-SILAR cycle variation on the physico-chemical as well as photoelectrochemical (PEC) performance of ZnO thin films has been investigated. The M-SILAR deposited ZnO thin films has been directly used as photoanode in the dye-sensitized solar cell (DSSCs). The DSSC prepared using ZnO photoelectrode deposited for 150 M-SILAR cycles,sensitized with N3 dye showed a power conversion efficiency (PCE) of 0.58%.

Keywords:M-SILAR Method, Dye-sensitized solar cell, N3 dye, Power conversion efficiency of 0.58%.

1. Introduction

Third generation solar cells gained a great breakthrough since Prof. Gratzel put forward the concept of dye-sensitized solar cell (DSSC) [1]. With ruthenium (Ru) based dyes and iodide-triiodide redox couple, power conversion efficiency (PCE) of 11.5% is achieved so far [2]. In the past two decades, a large number of binary metal oxides such as TiO_2, ZnO, Fe_2O_3, ZrO_2 and Nb_2O_5 have been tested for their use as photoelectrode in DSSCs. Among them, TiO_2 is the best candidate due to its favorable electronic band structure and recombination probability [3]. ZnO is also considered as a potential substitute for TiO_2 photoelectrode because of its similar electron affinity and a wide band gap of 3.37 eV. Also, it possesses higher bulk mobility indicating lower charge recombination [4]. Furthermore, different nanostructures of ZnO can be formed[5]. These nanostructures like nanoparticles, nanorods, nanosheets, nanowires, nanoflowers, tetrapods etc. are obtained by different physical as well as chemical routes such as and chemical vapor deposition (CVD), chemical bath deposition (CBD), spray pyrolysis, hydrothermal, electrodeposition and successive ionic layer adsorption and reaction (SILAR)[6-12]. Among these various methods, SILAR method is simple, non-toxic and offers low cost, large area deposition as compared to other solution based non-vacuum methods [13]. The thickness, composition and phase purity of thin films can be easily controlled merely by adjusting the growth parameters such as adsorption and reaction time, deposition cycles and precursor concentration [14].

The bottleneck for achieving high PCE is the competition between the generation and recombination of photoexcited carriers. In DSSC, a dense array of the one-dimensional (1D) nanostructure is of great importance as it allows large surface area and is able to provide the direct pathway for rapid collection of photogenerated electrons and, therefore, reduce the degree of

recombination [15,16]. Kumar et al. [8] have achieved the highest PCE of 1.1% with Ru-based N719 sensitizer with ZnO nanorods deposited by CBD with seed layer treatment. Hsu et al. [17] prepared the ZnO nanorods for solar cell and reported the highest PCE of 0.22% for hydrothermal and 0.18% for CVD method using N719 sensitizer. Baviskar et al. [18] obtained ZnO thin films by wet chemical synthesis using hexamethylenetetramine (HMTA) and ammonia as complexing agents with the deposition time of 40 h and achieved the PCE of 0.34% using N3 sensitizer. Pawar et al. [19] developed the ZnO bottle brush by applying double seed layer by reflux method and obtained the relatively highest PCE of 1% with N3 sensitizer. These synthetic methods are much time consuming and have to be operated at the higher temperature. Therefore using simple modified successive ionic layer adsorption and reaction (M-SILAR) method, nanostructured photoelectrodes can be directly fabricated with less deposition time.

In the present study, ultrasonic rinsing mediated M-SILAR method is employed for the deposition of ZnO thin films, which allows a good control on the growth of the ZnO thin films. Surfactant-free 1D ZnO microstructure has been grown without seed layer treatment by changing the M-SILAR cycles and their influence on the PEC properties of DSSC has been investigated.

2. Experimental

2.1 Chemicals

Zinc nitrate hexahydrate ($Zn(NO_3)_2.6H_2O$), ammonia (NH_4OH), hydrogen peroxide (H_2O_2), hexachloroplatinic acid ($H_2PtCl_6.6H_2O$) and cis-Bis(isothiocyanato)bis(2,2′-bipyridyl-4,4′-dicarboxylato)ruthenium(II) i.e. N3 dye, Acetonitrile, Hexachloroplatinic acid, 2-propanol, lithium iodide and iodinewere purchased from Aldrich. All reagents were used as received. Aqueous solutions were furnished using double distilled water (DDW).

2.2 Deposition of ZnO by M-SILAR method

ZnO thin films have been deposited using zinc-ammonia complexed precursor as cationic source and diluted hydrogen peroxide (H_2O_2) kept at 353 K temperature as an anionic sourcewith slight modifications in our previously reported procedure [20]. ZnO thin films have been grown on the soda-lime glass (SLG) and fluorine-doped tin oxide (FTO) coated glass substrates. The schematic setup used for M-SILAR deposition of ZnO thin films is shown in Figure 1. A complete deposition cycle to deposit ZnO thin films includes four steps: (1) the ultrasonically cleaned glass substrate was immersed in alkaline zinc nitrate solution, so that zinc complex adsorbs onto the substrate surface, (2) rinsing of substrate in DDW removes loosely bound particles from the substrate, (3) immersion of substrate into the dilute H_2O_2 (1%) kept at 353 K, the desired reaction occurred at substrate surface to form ZnO, (4) the ultrasonic rinsing of substrate in a separate beaker removes loosely bounded ZnO particles. The uniform and adherent deposition is observed when the adsorption and reaction time was 20s. This procedure was repeated successively for 50, 100, 150 and 200 times. The as-deposited films were annealed at 673 K in an air for 1 h to improve crystallinity and to remove the hydroxide phase. The films are denoted as ZO_{50}, ZO_{100}, ZO_{150} and ZO_{200} for 50, 100, 150 and 200 deposition cycles, respectively.

2.3 Fabrication of DSSC

ZnO films have been soaked in ethanolic 0.3 mM N3 dye solution at room temperature for 12 h and then washed carefully in ethanol, subsequently rinsed in acetonitrile and dried in an air. Compact DSSCs have been fabricated using a typical two electrode configuration with an active area of 0.25 cm^2. Dye-loaded ZO_{50}, ZO_{100}, ZO_{150} and ZO_{200} samples have been used as photoelectrode and platinum (Pt) coated FTO as the counter electrode. The counter electrode is prepared by simple drop cast method using the 10 mM $H_2PtCl_6.6H_2O$ in 2-propanol solution on the pre-drilled FTO and annealing at 723 K for 10 min. The two electrodes have been assembled using a thermoplastic (1mm). The space between the electrodes is filled with an electrolyte consisting of 0.1 M lithium iodide and 0.05 M iodine in acetonitrile through the predrilled hole in the counter electrode.

2.4 Characterization techniques

The structural properties of M-SILAR deposited ZnO samples with varying M-SILAR cycles is studied by using X-ray diffractometer (XRD) (Philips, PW 3710, Holland) operated at 40 kV, 30 mA with Cu K_α radiation (λ = 1.5406 Å) and Raman spectra is recorded using Raman microscope (LabRam, HR800 UV-Raman microscope (Horiba Jobin-Yvon, France) with excitation wavelength of 514 nm using diode laser. The surface morphology is observed using field emission scanning electron microscopy (FE-SEM) (Model Hitachi S4800, Japan.). The elemental composition of the deposited material was analyzed by energy dispersive X-ray spectrometer (EDAX) (Bruker, nano GmbH, Germany, attached to the FESEM). UV-visible absorbance spectra of the samples have been obtained by means of a UV-visible spectrophotometer (UV1800, Shimadzu, Japan). J-V curves have been recorded on the solar simulator (model CT- 150 AAA, photoemission tech, USA) under an Air Mass 1.5 G solar irradiation. Electrochemical impedance spectra (EIS) have been measured using electrochemical workstation (AUT8584) within the frequency range of 10 KHz to 10Hz.

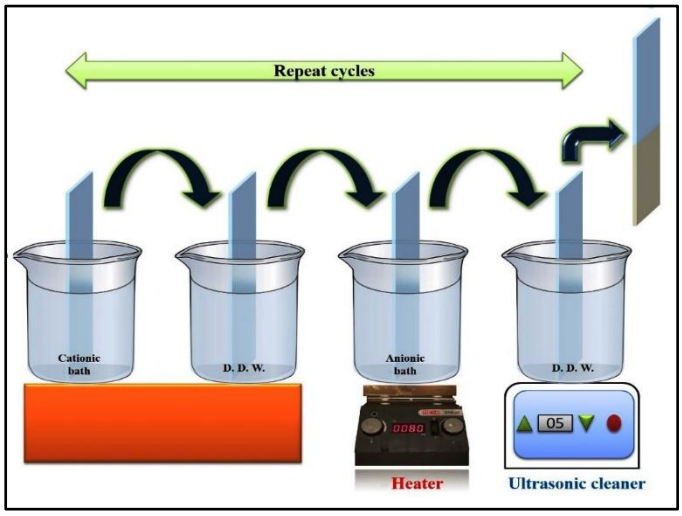

Figure 1: Schematic representation of modified SILAR (M-SILAR) method used to deposit ZnO thin films

3. Results and discussion

3.1 Reaction mechanism

The mechanism of ZnO film formation by M-SILAR method can be explained as follows: 0.1 M $Zn(NO_3)_2$ was used as a source of zinc and the pH was adjusted to 12 by dropwise addition of aqueous ammonia solution with constant stirring. Initially, when aqueous ammonia solution was mixed in the zinc nitrate solution, the ionic product of $Zn(OH)_2$ exceeds the solubility product and the solution turn out to be milky turbid due to the formation of $Zn(OH)_2$. This can be explained by the following reactions:

$$\mathbf{Zn(NO_3)_2 + 2NH_4OH \rightarrow Zn(OH)_2 + 2NH_4^+ + 2NO_3^-} \quad (1)$$

However, further addition of excess ammonia solution reduces Zn^{2+} ions by producing the complex ions of the type $Zn(NH_3)_n^{2+}$, which avoids precipitation and makes solution clear and transparent. This can be explained by the following reaction:

$$\mathbf{Zn(OH)_2 + 4NH_4^+ \rightarrow Zn(NH_3)_4^{2+} + 2H_2O + 2H^+} \quad (2)$$

When the substrate is immersed in the above solution, the zinc complex ions getting adsorbed on the substrate due to the attractive force between ions in the solution and surface of the substrate. The forces responsible for making the desired ZnO films may be cohesive forces or Van-der-Waals forces or chemical attractive forces [20]. The substrate is now immersed in dilute H_2O_2 solution, which is kept at 353 K to transform the zinc complex into ZnO by the reactions, which can be represented as:

$$\mathbf{H_2O_2 + H_2O \rightarrow 2\,OH^- + 2H^+ + {}^1/_2\,O_2} \quad (3)$$

$$\mathbf{Zn(NH_3)_4^{2+} + 2\,OH^- \rightarrow ZnO + 4NH_3 + H_2O} \quad (4)$$

In this case, dilute H_2O_2 solution acts as source of hydroxyl ions ($2OH^-$), which can also be obtained by heating of DDW at temperature near the boiling point [21]. As soon as the zinc complex coated substrate is dipped in the anionic bath, which is kept at 353 K, H_2O_2 instantaneously oxidizes the metal ions (Zn^{2+}), since it is extremely strong oxidizing mediator. The as deposited ZnO films are found to be homogeneous and well adherent to the substrate.

3.2 X-Ray diffraction study

Figure 2 shows the XRD patterns of ZO_{50}, ZO_{100}, ZO_{150} and ZO_{200} samples. All the ZnO samples exhibit the polycrystalline nature having foremost peak analogous to (002) plane as the highest intense peak. Other peaks corresponding to (100), (101), (103) and

(004) planes are observed (JCPDS card no. 00-003-0888). The relatively higher intensity of (002) diffraction peak provides evidence that the microstructure is preferentially oriented along c axis direction [22]. The crystallite size is calculated using Scherrer's formula $D = \frac{0.9\,\lambda}{\beta \cos\theta}$ and found to be 25, 29, 33 and 30 nm for ZO_{50}, ZO_{100}, ZO_{150} and ZO_{200} samples, respectively [23].

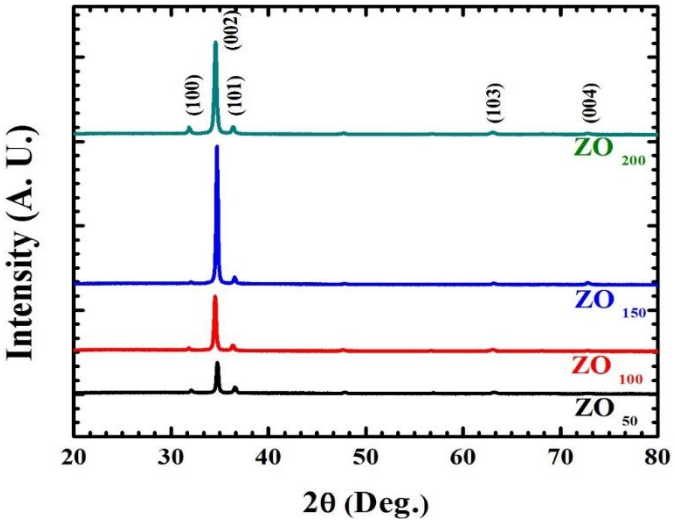

Figure 2: XRD patterns of ZO_{50}, ZO_{100}, ZO_{150} and ZO_{200} samples prepared by using different M-SILAR cycles

3.3 Raman spectroscopy:

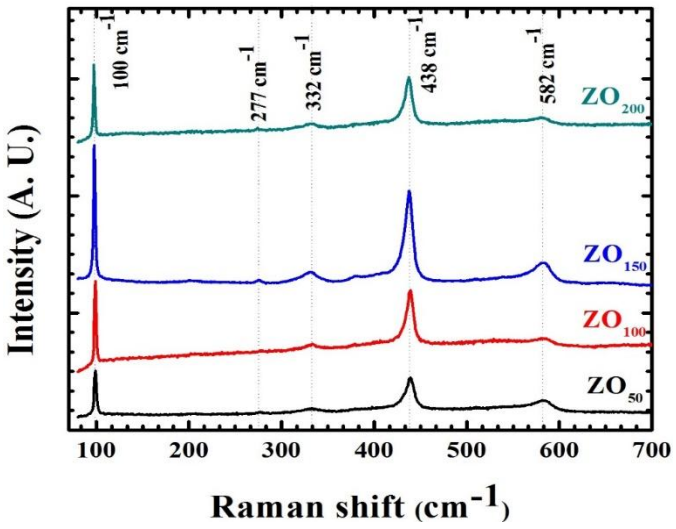

Figure 3: Raman spectra of ZO_{50}, ZO_{100}, ZO_{150} and ZO_{200} samples prepared by using differentM-SILAR cycles

The existence of phase pure ZnO is further confirmed by the Raman spectroscopy (Figure 3). All samples exhibit the strong peaks at 100 cm^{-1} and 438 cm^{-1} which correspond to heavy zinc sublattice vibration and oxygen atom vibration, respectively. The additional peaks observed at 277 cm^{-1} and 332 cm^{-1} are attributed to silent mode of wurtzite-ZnO (w-ZnO) and second order non polar mode arising from zone boundary phonons. The peak at 582 cm^{-1} is related to defects such as oxygen vacancy or interstitial zinc in zinc oxide. Thus, the observed peaks strongly support the formation of w-ZnO [24, 25].

3.4 Field emission scanning electron microscopy (FE-SEM):

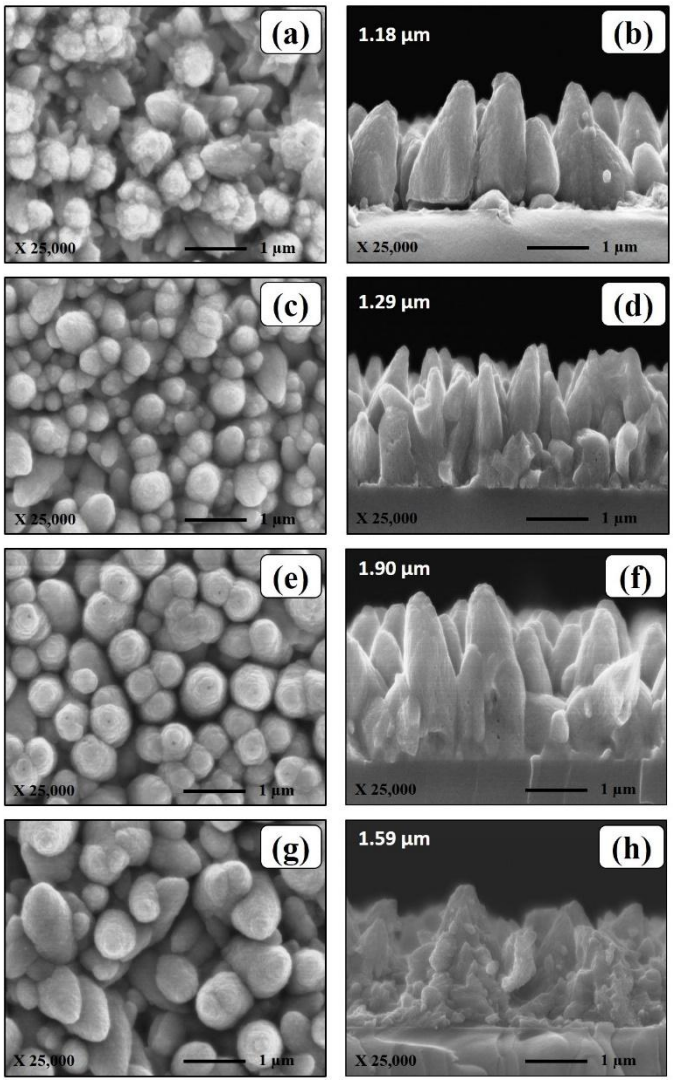

Figure 4: Surface and cross-sectional FE-SEM images of ZO_{50} (a and b), ZO_{100} (c and d), ZO_{150} (e and f) and ZO_{200} (g and h) samples prepared by using differentM-SILAR cycles

Figure 4(a-h) shows the surface and cross sectional FE-SEM images of ZO_{50}, ZO_{100}, ZO_{150} and ZO_{200} samples, respectively. As M-SILAR cycles increases, the thickness increases from 1.18 µm for ZO_{50} sample to 1.90 µm for ZnO_{150} sample and further reduces to 1.59 µm for ZO_{200} sample. The growth of the nuclei on substrate occurs by diffusion of clusters and coalescence of these clusters gives rise to the formation of a uniform film. As M-SILAR cycle increases, the growth of particles occurs on earlier grown nuclei and film thickness increases. After certain cycles, stress to the substrate due to growing number of clusters increases, which leads to peeling off the film from the substrate surface hence film thickness decreases[26]. As clearly seen from Figure 4(e, f), the resultant nanostructure is grown perpendicular to the substrate surface and densely cover the substrates.

In M-SILAR method, the ultrasonic rinsing instead of the mere mechanical rinsing by water leads to enhance the uniformity of the film. It is expected that the ultrasonic rinsing is not only functioning as a more efficient rinsing measure but also modify the deposition process of ZnO thin films andpromotes the quality deposition of the films by the use of cavitation effect [27]. Such uniform morphology is more beneficial in solar cell application as recombination rates of the photogenerated electron will be reduced [28].

3.4 Energy dispersive X-ray (EDAX) analysis

Figure 5 shows the EDAX spectrum of M-SILAR deposited ZO_{150} sample. Only Zn and O signals have been detected, which indicated that the nanostructure is indeed made up of Zn and O.

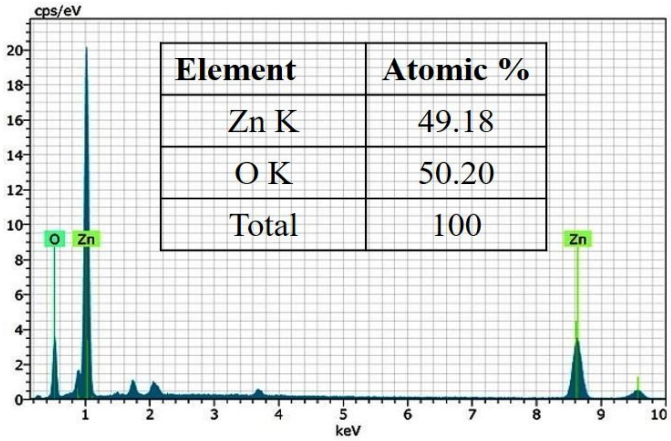

Element	Atomic %
Zn K	49.18
O K	50.20
Total	100

Figure 5:EDAX spectrum of typical optimized ZO_{150} sample prepared with 150 M-SILAR cycles

No signal of secondary phase or impurity is detected, indicating high purity of ZnO microstructure.The atomic percentage ratio is found to be nearly equal to one, showing sample is stoichiometric in the composition[29].

3.5 Optical Study:

Figure 6 shows the optical absorption spectra of dye-loaded ZO_{50}, ZO_{100}, ZO_{150} and ZO_{200} samples and ZO_{150} sample without dye loading (Figure 6(e)). The spectra revealed that the ZnO films have low absorbance in the visible region, which is characteristics of ZnO, however maximum absorption peak around 500 nm is seen with broader coverage in the visible region of the solar spectrum after dye-loading. The increased absorption near 500 nm is due to the sensitization of N3 dye. So, dye sensitization process shifts the absorbance of ZnO samples from UV to visible region, which is the key parameter in improving the PCE of DSSCs[30].

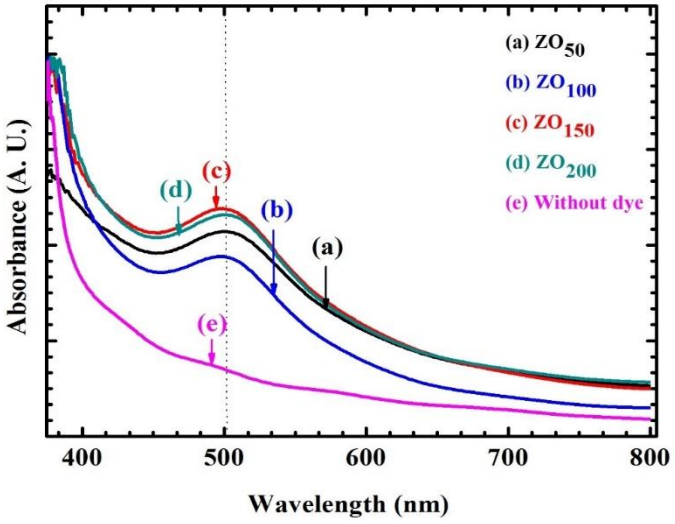

Figure 6: Absorbance Vs. wavelength spectra of dye-loaded (a) ZO_{50}, (b) ZO_{100}, (c) ZO_{150} and (d) ZO_{200} samples with different M-SILAR deposition cycles. (e) denotes the absorbance curve of ZO_{150} sample without dye loading.

3.6 J-V measurement:

Figure 7 (A) shows the idyllic diode behavior with a rectifying ratio communicating from the formation of a

junction between the ZnO photoelectrode and electrolyte. Figure 7 (B) shows the photocurrent density versus voltage (J-V) curves upon illumination of the DSSCs prepared using ZO_{50}, ZO_{100}, ZO_{150} and ZO_{200} samples, respectively.

Table 1 shows various solar cell parameters for the DSSCs, where J_{sc} is the short circuit current density, V_{oc} is the open-circuit voltage, FF is the fill factor, η is the PCE.It is observed that J_{sc} along with FF goes on increasing with increase in thickness of the samples ZO_{50} to ZO_{150}.

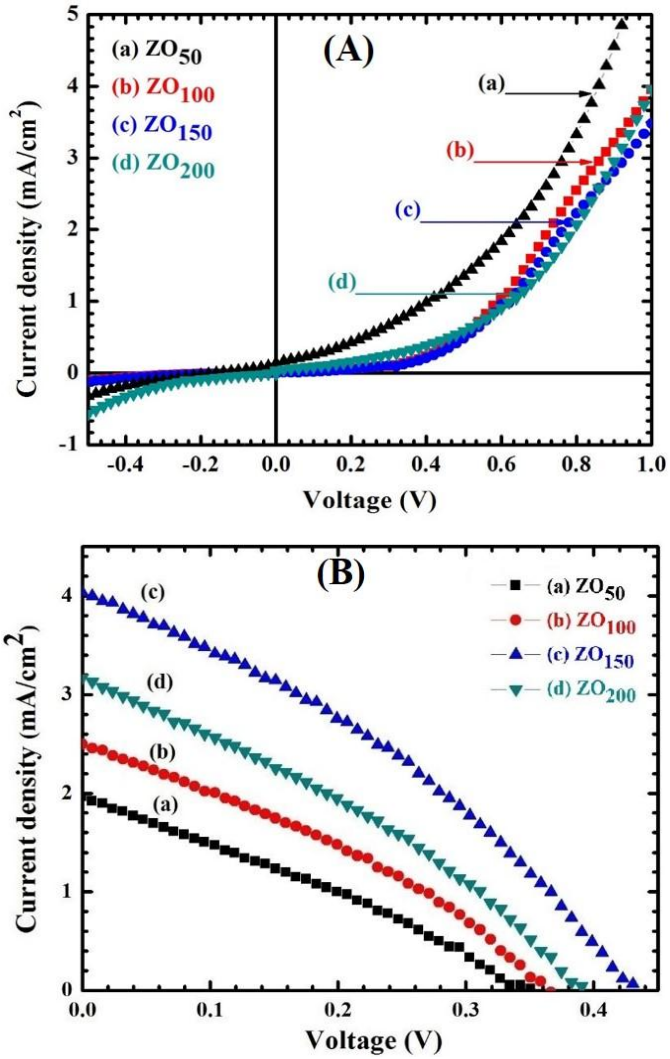

Figure 7: Photocurrent density- voltage (J-V) curves (A) in dark and (B) upon illumination for DSSCs prepared using (a) ZO_{50}, (b) ZO_{100}, (c) ZO_{150} and (d) ZO_{200} samples with different M-SILAR cycles

Table 1: Performance of the ZO_{50}, ZO_{100}, ZO_{150} and ZO_{200} samples determined by photocurrent density- voltage (J-V) characteristics

Sample	Thickness (μm)	J_{sc} (mA/cm^2)	V_{oc} (V)	FF	PCE (η) (%)
ZO_{50}	1.18	1.96	0.34	0.29	0.19
ZO_{100}	1.29	2.48	0.36	0.32	0.29
ZO_{150}	1.90	4.02	0.43	0.33	0.58
ZO_{200}	1.59	3.12	0.39	0.31	0.38

DSSC prepared using ZO_{150} sample has the highest PCE of 0.58%, with the J_{sc} of 4.02 mA/cm^2 and V_{oc} of 0.43 V. This device contributes highest J_{sc} due to the well-defined 1D microstructure which allows high internal surface area for dye adsorption and facilitates pathway for easy electron transport through them (Figure 4(e, f)).

3.7 EIS study:

Electrochemical impedance spectroscopy (EIS) has been used to understand the complex kinetics of charge transport, electronic and ionic processes in photoelectrochemical (PEC) solar cell [31]. EIS measurement of all the ZnO samples has been conducted in the dark using an iodide- triiodide electrolyte with applied forward bias voltage of 100 mV within the frequency range of 10 kHz to 10 Hz. EIS spectra of PEC solar cell generally exhibit three arcs, which are related to charge transfer resistance at counter electrode (Pt-FTO)/electrolyte interface (R_1), charge transfer resistance at photoelectrode/electrolyte interface (R_2) and Warburg impedance (Z_w) describing the diffusion of I_3^- in the electrolyte. R_s is the series resistance or solution resistance [32]. Figure 8 (A)shows the Nyquist plots of DSSCs prepared using ZO_{50}, ZO_{100}, ZO_{150} and ZO_{200} samples and Figure 8 (B) shows the equivalent circuit model used to analyze the EIS data and transport parameters of the electrons in the above samples.It is seen from Table 2 that R_1 and R_2 go on decreasing with increase in the thickness of the ZnO samples. Sample ZO_{150} has R_1 = 66.8 Ω/cm^2 and R_2 = 97.1 Ω/cm^2, which are much lower than rest of ZnO samples. A likely reason for this phenomenon is that more electrons were shot up into the conduction band of ZnOnanostructure, which is in accordance with the increase in J_{sc} values [33]. This indicates that sample ZO_{150} is more conducting than other samples,

which is thereby producees highest values of J_{sc} and V_{oc} upon illumination.

To calculate electron lifetime (τ_e), Bode plot (Figure 8 (C)) is used which can be obtained from EIS data by plotting the graph between phase versus log (F). The τ_e is calculated using the formula, $\tau_e = 1/ 2\pi F_{max}$[34]. The maximum frequency peaks for ZO_{50}, ZO_{100}, ZO_{150} and ZO_{200} samples are at 0.69 KHz, 1.86 KHz, 2.23 KHz and 3.54 KHz, respectively.

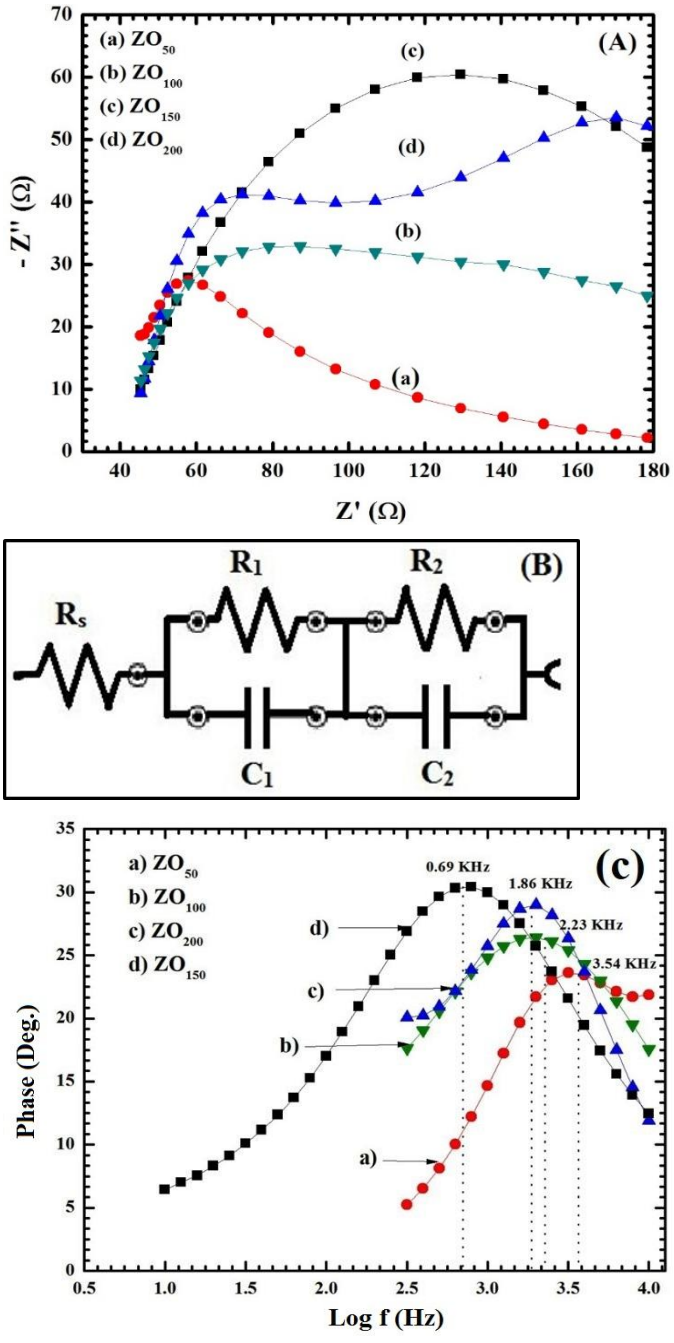

Figure 8: (A) Nyquist plots, (B) equivalent circuit model used to analyze the EIS data and (C) Bode plots of DSSCs prepared using (a) ZO_{50}, (b) ZO_{100}, (c) ZO_{150} and (d) ZO_{200} samples

Maximum τ_e is found to be 93 µs for ZO_{150} sample, as it possesses relatively superior microstructure and thus provides the effective pathway to the photogenerated electrons with low recombination rate. From EIS results, it is clear that the determination of charge recombination rate is the key parameter of ZnO DSSC performance. Thus, it is concluded that charge recombination of ZO_{150} sample is lower than other samples and, thus, it gives the highest PCE of 0.58%.

Table 2: Electron transport properties of the ZO_{50}, ZO_{100}, ZO_{150} and ZO_{200} samples determined by electrochemical impedance spectroscopy (EIS) analysis

DSSC	R_s (Ω/cm^2)	R_1 (Ω/cm^2)	R_2 (Ω/cm^2)	τ_e (µs)
ZO_{50}	44.7	170	497	44
ZO_{100}	43	150	178	71
ZO_{150}	41	31	26	93
ZO_{200}	42.2	70.6	101	85

Conclusions

ZnO thin films have been deposited by using M-SILAR method. M-SILAR deposited photoelectrodes have been incorporated into DSSCs where they display reasonable light-harvesting efficiency, better photocurrent and photovoltage with good fill factor. It is observed that the thickness significantly affects the physico-chemical and PEC properties of ZnO samples. The DSSC with ZO_{150} sample having thickness of 1.9 µm exhibits the highest PCE of 0.58 % with J_{sc} of 4.02 mA/cm^2 and V_{oc} of 0.43 V.

Acknowledgements

Authors wish to acknowledge the DAE- BRNS, Mumbai, India for financial support through major research project (No. 2013/36/29-BRNS/2351) and KBSI, Gwangju-center, South Korea for Raman and FE-SEM facility.

References:

[1] B. O'Regan, M. Gratzel, "A low-cost, high-efficiency solar cell based on dye-sensitized colloidal TiO_2 films", Nature,353(1991)737

[2] C. Y. Chen, M. Wang, J. Y. Li, N. Pootrakulchote, L. Alibabaei, C. Ngoc-le, J. D. Decoppet, J. H. Tsai, C. Gratzel, C. G. Wu, S. M. Zakeeruddin, M. Gratzel, "Highly efficient light-harvesting ruthenium sensitizer for thin-film dye-sensitized solar cells",ACS Nano, 3(2009)3103

[3] R. Jose, V. Thavasi, S.Ramakrishna, "Metal oxides for dye sensitized solar cells", J. Am. Ceram. Soc., 92 (2009)289

[4] Y. M. Lee andH. W. Yang,"Optimization of processing parameters on the controlled growth of ZnO nanorod arrays for the performance improvement of solid-state dye-sensitized solar cells",J. Solid State Chem., 184 (2011)615

[5] Z. L. Wang,"Zinc oxide nanostructures: growth, properties and applications",Mater. Today, 7 (2004) 26

[6] C. Y. Lin, Y. H. Lai, H. W. Chen, J. G. Chen, C. W. Kung, R. Vittal, K. C. Ho,"Highly efficient dye-sensitized solar cell with a ZnO nanosheet-based photoanode", Energy Environ. Sci.,4 (2011) 3448

[7] K. Ravichandran, P. V. Rajkumar, B. Sakthivel, K. Swaminathan, L. Chinnappa, "Role of precursor material and annealing ambience on the physical properties of SILAR deposited ZnO films",Ceramics International, 40 (2014) 12375

[8] R. S. Kumar, P. Sudhagar, P. Matheswaran, R. Sathyamoorthy, Y. S. Kang, "Influence of seed layer treatment on ZnO growth morphology and their device performance in dye-sensitized solar cells", Mater. Sci. Eng., B, 172 (2010) 283

[9] W. Yang, F. Wan, S. Chen, C. Jiang, "Hydrothermal growth and application of ZnO nanowire films with ZnO and TiO 2 buffer layers in dye-sensitized solar cells",Nanoscale Res. Lett., 4 (2009) 1486

[10] H. Muguerra, G. Berthoux, W.Z. N. Yahya, Y. Kervella, V. Ivanova J. Bouclé, R. Demadrille, "Electrodeposited ZnO nanowires as photoelectrodes in solid-state organic dye-sensitized solar cells",Phys. Chem. Chem. Phys., 16 (2014) 7472

[11] K. Mahmood and S. B. Park, "Highly efficient dye-sensitized solar cell with an electrostatic spray deposited upright-standing boron-doped ZnO (BZO) nanoporous nanosheet-based photoanode", J. Mater. Chem. A, 1.15 (2013) 4826

[12] L. Lu, J. Chen, L. Li, W. Wang, "Hydrothermal synthesis of MnO_2/CNT nanocomposite with a CNT core/porous MnO_2 sheath hierarchy architecture for supercapacitors",Nanoscale Res. Lett., 7.1 (2012) 1

[13] H. Li, S. Jiao, J. Ren, H. Li, S. Gao, J. Wang, D. Wang, Q. Yu, Y. Zhang, L. Li, "Reaction mechanism of a PbS-on-ZnO heterostructure and enhanced photovoltaic diode performance with an interface-modulated heterojunction energy band structure", Phys. Chem. Chem. Phys., 18 (2016)4144

[14] M. P. Suryawanshi, P. S. Patil, S. W. Shin, K. V. Gurav, G. L. Agawane, M. G. Gang, J. H. Kim, A. V. Moholkar, "The synergistic influence of anionic bath immersion time on the photoelectrochemical performance of CZTS thin films prepared by a modified SILAR sequence",RSC Adv., 4 (2014) 18537

[15] J. B. Baxter and E. S. Aydil, "Nanowire-based dye-sensitized solar cells", Appl. Phys. Lett., 86.5 (2005) 053114

[16] I. G. Valls and M. L. Cantu, "Vertically-aligned nanostructures of ZnO for excitonic solar cells: a review", Energy Environ. Sci., 2 (2009) 19

[17] Y. F. Hsu, Y. Y. Xi, A. B. Djurisic, W. K. Chan, "Dye-sensitized solar cells using ZnO tetrapods", J. Appl. Phys., 103.8 (2008) 083114

[18] P. K. Baviskar, W. Tan, J. Zhang, B. R. Sankapal, "Wet chemical synthesis of ZnO thin films and sensitization to light with N3 dye for solar cell

application", J. Phys. D: Appl. Phys., 42.12 (2009) 125108

[19] R. C. Pawar, J. S. Shaikh, P. S. Shinde, P. S. Patil, " Low temperature aqueous chemical synthesis of CdS sensitized ZnO nanorods", Mater. Lett., 65.14 (2011) 2235

[20] M. A. Gaikwad, M. P. Suryawanshi, S. S. Nikam, C. H. Bhosale, J. H. Kim, A. V. Moholkar, "Influence of Zn concentration and dye adsorption time on the photovoltaic performance of M-SILAR deposited ZnO-based dye sensitized solar cells", J. Photochem. Photobiol., A, 329 (2016) 246

[21] V. R. Shinde, T.P. Gujar, C.D. Lokhande, "Studies on growth of ZnO thin films by a novel chemical method", Sol. Energy Mater. Sol. Cells 91.12 (2007)1055

[22] A. Arslan, E. Hur, S. Ilican, Y. Caglar, M. Caglar, "Controlled growth of c-axis oriented ZnO nanorod array films by electrodeposition method and characterization", Spectrochimica Acta Part A: Molecular and Biomolecular Spectroscopy, 128 (2014) 716

[23] S. P. Desai, M. P. Suryawanshi, S. M. Bhosale, J. H. Kim, A. V. Moholkar, "Influence of growth temperature on the physico-chemical properties of sprayed cadmium oxide thin films", Ceram. Int., 41.3 (2015) 4867

[24] D. Polsongkram, P. Chamninok, S. Pukird, L. Chow, O. Lupan, G. Chai, H. Khallaf, S. Park, A. Schulte, "Effect of synthesis conditions on the growth of ZnO nanorods via hydrothermal method",Physica B, 403.19 (2008) 3713

[25] M. L. Zhang, F. Jin, M. L. Zheng, J. Liu, Z. S. Zhaoa, X. M. Duan, "High efficiency solar cell based on ZnO nanowire array prepared by different growth methods", RSC Adv., 4 (2014) 10462

[26] I. Pushpitasari, T. P. Gujar, K. D. Jung, O. S. Joo, "Simple chemical preparation of CuS nanowhiskers", Mater. Sci. Eng., B, 140.3 (2007) 199

[27] X. D. Gao, X. M. Li, W. D. Yu, "Synthesis and optical properties of ZnO nanocluster porous films deposited by modified SILAR method", Appl. Surf. Sci., 229.1 (2004) 275

[28] M. Skompska and K. Zarebska, "Electrodeposition of ZnO nanorod arrays on transparent conducting substrates–a review", Electrochim. Acta 127 (2014) 467

[29] R. Mariappan, V. Ponnuswamy, P. Suresh, N. Ashok, P. Jayamurugan, A. C. Bose, "Influence of film thickness on the properties of sprayed ZnO thin films for gas sensor applications", Superlattices Microstruct., 71 (2014) 238

[30] P. Singh and N. M. Ravindra, "Temperature dependence of solar cell performance- an analysis", Sol. Energy Mater. Sol. Cells, 101 (2012) 36

[31] D. Sengupta, P. Das, B. Mondal, K. Mukherjee, "Effects of doping, morphology and film-thickness of photo-anode materials for dye sensitized solar cell application-A review", Renew. Sust. Energ. Rev., 60 (2016) 356

[32] Q. Wang, J. E. Moser, M. Gratzel, "Electrochemical impedance spectroscopic analysis of dye-sensitized solar cells", J. Phys. Chem. B, 109.31 (2005)14945

[33] C. P. Hsu, K. M. Lee, J. T. W. Huang , C.Y. Lin , C.H. Lee, L. P. Wang, S. Y. Tsai, K. C. Ho, "EIS analysis on low temperature fabrication of TiO_2 porous films for dye-sensitized solar cells", Electrochim. Acta 53.25 (2008) 7514

[34] G. Dai, L. Zhao, J. Li, L. Wan, F. Hu, Z. Xu , B. Dong, H. Lu, S. Wang, J. Yu, "A novel photoanode architecture of dye-sensitized solar cells based on TiO_2 hollow sphere/nanorod array double-layer film", J. Colloid Interface Sci., 365.1 (2012) 46